Coupling 3D hydraulic simulation and fish telemetry data to characterize the behavior of migrating smolts approaching a bypass

Noor Ben Jebria, Rémi Arthur Carmigniani, Hilaire Drouineau, Eric de Oliveira, Stéphane Tétard, Hervé Capra

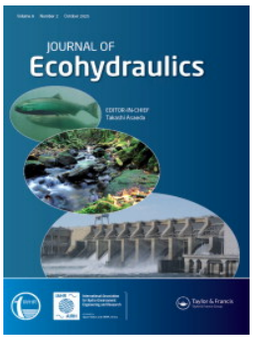

Journal of Ecohydraulics

ISSN: (Print) (Online) Journal homepage: https://www.tandfonline.com/loi/tjoe20

Coupling 3D hydraulic simulation and fish telemetry data to characterize the behaviour of migrating smolts approaching a bypass

Noor Ben Jebria, Rémi Carmigniani, Hilaire Drouineau, Eric De Oliveira, Stéphane Tétard & Hervé Capra

To cite this article: Noor Ben Jebria, Rémi Carmigniani, Hilaire Drouineau, Eric De Oliveira, Stéphane Tétard & Hervé Capra (2023) Coupling 3D hydraulic simulation and fish telemetry data to characterize the behaviour of migrating smolts approaching a bypass, Journal of Ecohydraulics, 8:2, 144-157, DOI: 10.1080/24705357.2021.1978345

To link to this article: https://doi.org/10.1080/24705357.2021.1978345

Published online: 12 Oct 2021.

JOURNAL OF ECOHYDRAULICS
2023, VOL. 8, NO. 2, 144–157
https://doi.org/10.1080/24705357.2021.1978345

Coupling 3D hydraulic simulation and fish telemetry data to characterize the behaviour of migrating smolts approaching a bypass

Noor Ben Jebria[a], Rémi Carmigniani[b], Hilaire Drouineau[c], Eric De Oliveira[a], Stéphane Tétard[d] and Hervé Capra[e]

[a]EDF R&D LNHE - Laboratoire National d'Hydraulique et Environnement, HYNES (INRAE-EDF R&D), Chatou, France;[b]LHSV, Ecole des Ponts, CEREMA, EDF R&D, Chatou, France; [c]INRAE, Unité EABX – Écosystèmes Aquatiques et Changements Globaux, HYNES (INRAE-EDF R&D), Cestas Cedex, France; [d]ICEO, Talmont Saint Hilaire, France; [e]INRAE, RiverLy, Villeurbanne Cedex, France

ABSTRACT

Human-induced river fragmentation is a major threat to migratory fish species. Restoring river connectivity requires the construction of fish passage solutions, such as fishways for upstream and downstream migration. While many studies focussed on the upstream migration of diadromous fishes, and especially of adult Atlantic salmons (*Salmo salar*), we analyze juvenile behaviour under different hydraulic conditions at reservoir to improve the development of effective bypass systems for downstream passage of salmon smolt.

Based on coupling three-dimensional (3D) computational fluid dynamics (CFD) simulations to smolt positions tracked by two-dimensional (2D) telemetry, the present study aimed to explore smolt behaviour in relation to hydraulic cues. More specifically, we explored how hydraulic conditions influence fish behaviour and how fish navigate depending on this behaviour. In 2017, 23 smolts were tracked in the reservoir of Poutès (Allier River, France), associated with different turbine discharge rates. 3D CFD simulations were performed and validated against field measurements in the reservoir upstream of the hydropower plant.

The study of fish displacements in relation to flow conditions provided new insights with the use of thrust force, swimming orientation and direction as means to precisely characterize smolt behaviour, which can help in the design of downstream migration passage facilities. At Poutès dam, flow velocity, flow acceleration and turbulent kinetic energy are very low and therefore can lead to fish disorientation. However, results underlined that having a minimum flow velocity of 20 cm/s in reservoirs is sufficient to prevent delay and allow fish navigation.

KEYWORDS

Computational fluid dynamics; *Salmo salar*; fish behaviour; downstream migration; swim path

1. Introduction

Ecosystem fragmentation is a major threat to biodiversity and one of the main challenges for the conservation and restoration of aquatic environments (Malmqvist and Rundle 2002; Strayer and Dudgeon 2010; Neeson et al. 2015). In aquatic ecosystems, human-induced longitudinal barriers, such as dams and weirs, are partly responsible for the decline in fish populations. The impact is even greater on diadromous species with life-cycles spanning marine and freshwater ecosystems. By blocking migration, river fragmentation is thought to be the main cause of the extinction of some populations or their confinement to restricted areas in river basins (Porcher and Travade 1992; Kondolf 1997; Coutant and Whitney 2000; Larinier 2001; Fukushima et al. 2007). Among human-induced obstacles to migration, hydropower plants pose an additional risk during migration: passage through turbines can cause direct injury and mortality (Baras and Lucas 2001; Larinier 2001; Thorstad et al. 2008; Limburg and Waldman 2009; Bunt et al. 2012). Some large dams also disorient migratory fish by affecting stream flow (Ovidio et al. 2016; Schwinn et al. 2019) and potentially delaying migration (McCormick 1998; Marschall et al. 2011).

One of the most common means of restoring the continuity of watercourses is fish passage solutions (FPS), with variable effectiveness (Noonan et al. 2012). Poor efficiency can sometimes result from unsuitable hydraulic conditions inside the FPS, but also from a lack of attractiveness for target species. Fish must locate the area influenced by the flow from the fishway to the FPS entrance (Groux et al. 2017). The development of effective fish passage therefore depends on understanding the behavioural response to hydraulic conditions that may attract or

CONTACT Noor Ben Jebria noor.ben-jebria@edf.fr EDF R&D LNHE - Laboratoire National d'Hydraulique et Environnement, HYNES (INRAE-EDF R&D), Chatou, France.

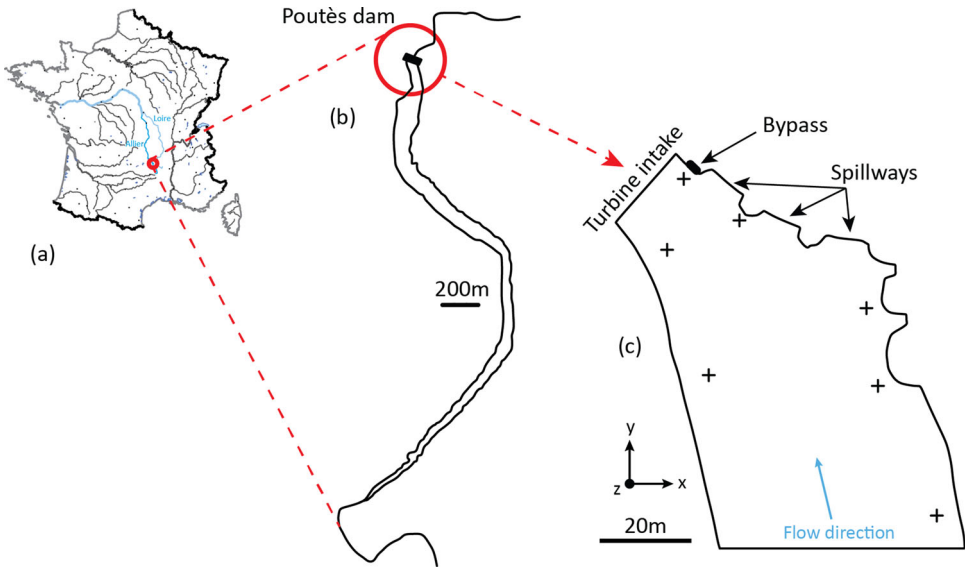

Figure 1. Study area of smolt migration: (a) location of the Allier River in France, (b) location of Poutès dam zone on the Allier River, (c) zoom on the dam and simulation zone. The crosses indicate hydrophone locations in 2017 (Tétard et al. (2021)).

repel fishes. While much attention has been paid to upstream passage solutions, knowledge is still lacking, especially for downstream passage (Larinier and Travade 2002; Williams et al. 2012; Silva et al. 2020).

It is well known that fish can sense variations in water pressure and velocity by means of their lateral line and inner ear (Dijkgraaf 1963; Kalmijn 1989; Montgomery et al. 1997; Braun and Coombs 2000; Montgomery et al. 2001; Bleckmann and Zelick 2009; Mogdans 2019). For juvenile Atlantic salmons (known as smolts) undertaking their seaward migration, changes in hydraulic conditions, as reflected in water velocity, turbulence and acceleration, provide the major cues in seeking the migration pathway (Haro et al. 1998; Liao et al. 2003; Liao 2007; Kemp et al. 2008; Tarrade et al. 2008; Enders et al. 2009; Johnson et al. 2009; Silva et al. 2011, 2012; Gao et al. 2016). However, it is less understood how fish respond to these stimuli. Studies showed that smolts tend to avoid areas with rapid changes in water velocity (Haro et al. 1998; Kemp et al. 2005, 2008; Enders et al. 2009) and are attracted towards flow with less turbulence and lower velocity and acceleration. Moreover, they tend to follow the bulk flow (Faber et al. 2001; Liao 2007; Evans et al. 2008; Williams et al. 2012). For smolts swimming in forebays close to turbines and bypass, where mean average flow velocities and turbulence intensities are higher, fish can experience disorientation. Therefore, they swim faster to diverge from the flow and displayed positive rheotaxis (tail-first; Haro et al. 1998; Enders et al. 2003, 2009; Silva et al. 2020).

Recent telemetry studies provided valuable information on fish migration routes during downstream migration and improved our understanding of migrating fish behaviour near dam structures (Jansen et al. 2007; Calles et al. 2010; Pedersen et al. 2012; Nyqvist, Greenberg, et al. 2017; Thorstad et al. 2017; Li et al. 2018). Coupled with hydraulic data, they provide insights into how hydraulic cues influence navigation in dam reservoir (Johnson et al. 2000; Faber et al. 2001; Johnson and Dauble 2006; Timko et al. 2007; Evans et al. 2008; Johnson et al. 2009; Steig and Johnston 2010; Khan et al. 2012; Arenas et al. 2015). Results show that as flow acceleration increases Pacific salmon smolts, steelhead trouts (Johnson et al. 2000; Faber et al. 2001; Evans et al. 2008; Johnson et al. 2009; Enders et al. 2009; Vowles et al. 2014; Arenas et al. 2015) and Atlantic salmon smolts (Szabo-Meszaros et al. 2019; Silva et al. 2020) tend to actively swim instead of drift, orient themselves against the flow and swim upstream. Moreover, the effort made by fish to resist the flow increases.

During the last decade, hydraulic models and fish behaviour models have been coupled to support the design of fish passages (Goodwin et al. 2006, 2014). However, most of these studies have focussed on large dam structures with high powerhouse discharge, such as the Columbia River hydroelectric plants in the United States (Haefner and Bowen 2002; Scheibe and Richmond 2002; Goodwin et al. 2006, 2014). Yet, less studies have been conducted on dams with large reservoirs and low powerhouse discharges, despite these sites higher prevalence for relatively quiescent flows known to disorient fish (Coutant and Whitney 2000).

In view of this, the present study aimed to analyze the effect of hydraulic conditions on Atlantic salmon smolt behaviour in a large reservoir upstream of a hydropower plant during their

downstream migration. The fish behaviour was characterized by their thrust forces. To compute these forces, fish velocities and hydraulic conditions encountered by the fish along their trajectories were evaluated. Acoustic telemetry combined with 3D computational fluid dynamics (CFD) modelling characterized smolt swimming behaviour in the reservoir under different hydraulic conditions. More specifically, we explored how hydraulic conditions influenced fish orientation in relation to flow direction, direction of the fish displacement and fish thrust force.

2. Materials and methods

2.1. General approach

In this study, we coupled 2D fish telemetry data with 3D CFD simulation results to better understand how the hydraulic conditions affected fish movement. Among all possible hydraulic variables provided by 3D CFD simulations, we focussed on time-average flow velocity, flow acceleration and turbulent kinetic energy (TKE) at each fish location because those variables proved to be important factors affecting fish behaviour (Haro et al. 1998; Liao 2007; Johnson et al. 2009; Gao et al. 2016). By combining fish trajectory (velocity and acceleration) and the physical forces acting on the fish (due to time-average flow velocity), fish thrust magnitude and orientation were determined by solving Newton's second law at every recorded fish location. This was used to explore the influence of hydraulic conditions on fish swimming behaviour.

2.2. Study area

The Poutès dam (France) is located 900 km from the Atlantic Ocean, on the Allier River, the main left-bank tributary of the Loire River (Figure 1). The Atlantic salmon has now disappeared from most of the major rivers of Europe but still migrates in the Loire-Allier River system, although the population has declined dramatically by around 80% in the late eighties (Cuinat 1988; Dauphin and Prévost 2013).

The dam is 85 m wide and 18 m high, equipped with three spillway gates (each 14 m long). The turbine intake is 24 m long and 5.7 m high. It is located on the left bank 7 m below the surface in normal operating conditions (water depth of 15.7 m). It is equipped with a trashrack with 3 cm bar spacing. It supplies three Francis turbines (1/2: 16 m^3 s^{-1}; 3 : 3 m^3 s^{-1}). It can deliver a maximum flow of 30 m^3 s^{-1} to the Monistrol powerhouse. A surface bypass is located upstream of the turbine intake on the left bank (Figure 1). It is operating during the salmon downstream migration period from March to June. It is mounted on a gate automatically regulated according to water level, to ensure a continuous bypass flow of 2 m^3 s^{-1}, representing 7.1% of the maximum turbine intake (Tétard et al. 2021).

2.3. Fish telemetry

To study the downstream movement of Atlantic salmon in the forebay of the Poutès dam, eleven WHS4000 hydrophones (Lotek Wireless Inc.) were positioned near the dam (see Figure 1, c): seven in the reservoir 80 m upstream of the dam and four in the bypass stretch 300 m downstream to confirm passage through the surface bypass. The system tracked fish in two dimensions with a median precision of 1.1 m (Tétard et al. 2021). The study is performed at water temperature of 6 to 10.9 °C (Tétard et al. 2019).

Two rotary screw traps were used to catch wild migrating fish, as described in Tétard et al. (2021). However, as the number of fish trapped was insufficient, some smolts from the National Wild Salmon Conservatory (CNSS) fish farm were used to ensure that a substantial number of fish were tagged.

In this study, 23 juvenile Atlantic salmon were tracked: 8 of them are wild fishes and 15 are from hatchery fish. In total, 1,618 positions were recorded (193 and 1,425 positions for wild and hatchery fish respectively). Mean total smolt length was $L_{sm} =$ 152 mm (152 ± 30 and 164 ± 9.7 mm for wild and hatchery fish respectively) and mean body weight $m_{sm} = 30.0$ g (28 ± 16 and 40 ± 7.4 g for wild and hatchery fish respectively) (Tétard et al. 2021).

For each fish, the average time between two detections was 5 sec (Tétard et al. 2021). The succession of a fish position through time allows the reconstruction of trajectories. When the time between two detections was greater than 37 sec, we considered the two locations as independent leading to two separate trajectories. This delay corresponds to the threshold after which two positions are not significantly autocorrelated. We observed a total of 134 trajectories (8 and 126 trajectories for wild and hatchery fish respectively).

2.4. CFD modelling

In order to get realistic information about the hydraulic conditions encountered by smolts while they travelled through the dam's reservoir, we used numerical simulations. The Reynolds-Averaged Navier Stokes (RANS) equations with $k-\epsilon$ turbulence model were solved using a finite volume method to obtain the three-dimensional components of velocity, pressure, TKE and the rate of turbulence dissipation. We used the open-source software Code Saturne

Table 1. Numerical simulations estimating hydraulic conditions encountered by smolts, and the number of smolts and smolt's positions observed.

		River		Powerhouse		Spillway			
Number of the numerical simulation	Water depth (*m*)	Discharge (m^2/s)	cross-sectional average velocity (m / s)	Discharge (m^2/s)	cross-sectional average velocity (m / s)	Discharge (m^2/s)	cross-sectional average velocity (m / s)	Number of smolts: total/wild	Number of smolt's positions: total/wild
1	11	29	0.12	15	0.42	14	1.25	3/0	85/0
2	11	40	0.17	27	0.76	13	1.16	2/2	145/145
3	11	78	0.33	30	0.85	48	1.2	6/6	48/48
4	15.7	7	0.029	2	0.056	5	0.45	7/0	766/0
5	15.7	15	0.063	10	0.28	5	0.45	5/0	574/0

(version 6.0, R&D EDF 2015) for the 3D simulations of the flow in the Poutès forebay.

Boundary conditions based on 2017 hydrology data were used to assign a fixed flow rate and water elevation to the entrance and exit of the system (bypass and turbine intake). Flow rate values for each configuration are listed in Table 1. As we expected little surface deformation and discounted wind effects on the flow, we modelled the free surface using a homogeneous Neumann for the scalar fields and a zero Dirichlet for the vector fields. In other words, the surface behaved like a symmetric plane or mirror in the simulations. The remaining boundaries were assumed to be rough walls with default roughness height of 0.01 m.

The 3D mesh was built using the open-source Salomé software (version 8.3.0), based on the planes provided by the operator. The mesh was constituted of 6×10^5 hexaedric elements of variable size (varying from 20 cm near the turbine intake and the spillway gates, to about 2 m in the reservoir). A convergence study was performed to validate the simulation. We verified that the refined mesh did not change flow velocity at fish positions. We concluded that this resolution was sufficient to get realistic information on the flow.

Numerical simulations were run with constant flow rate conditions, letting the simulations converge to a steady state. The simulations were performed using 56 CPUs; computational time to steady state was approximately 30 minutes.

Numerical simulations allowed us to evaluate the hydraulic variables influencing smolt behaviour at each position. The module of the total acceleration was calculated as:

$$a_f(x,y,z) = \sqrt{(a_x)^2 + (a_y)^2 + (a_z)^2}$$

where $a_x = u\left(\frac{\partial u}{\partial x}\right) + v\left(\frac{\partial u}{\partial y}\right) + w\left(\frac{\partial u}{\partial z}\right)$, $a_y = u\left(\frac{\partial v}{\partial x}\right) + v\left(\frac{\partial v}{\partial y}\right) + w\left(\frac{\partial v}{\partial z}\right)$ and $a_z = u\left(\frac{\partial w}{\partial x}\right) + v\left(\frac{\partial w}{\partial y}\right) + w\left(\frac{\partial w}{\partial z}\right)$ are the components of the flow acceleration a_f along x, y and z, respectively and u, v, w are the velocity components along x, y and z, respectively. Hereafter, we call $\vec{u}_f$ the time-average velocity and the subscript f designates the fluid. The module of the time-average velocity u_f was calculated as:

$$u_f(x,y,z) = \sqrt{(u)^2 + (v)^2 + (w)^2}$$

where u, v and w are the components of flow velocity along x, y and z.

The turbulent kinetic energy k is the mean kinetic energy per unit mass associated with vortices in a turbulent flow. It is calculated as:

$$k = \frac{1}{2}((u')^2 + (v')^2 + (w')^2)$$

It corresponds to half the sum of the variances of the velocity of fluctuation. Where u' the velocity of fluctuation is the difference between the instantaneous velocity u and the average velocity; $\vec{u}' = \vec{u} - \vec{\bar{u}}$ and $\vec{\bar{u}} = \vec{u}_f$.

The different numerical simulations to estimate the hydraulic conditions encountered by the fish at Poutès during telemetry measurement in 2017 are listed in Table 1. For simplification, only fish measurements during steady hydraulic conditions were analyzed. Since we only had 2D telemetry data, we assumed that fish swim two meters below the water surface.

2.5. Validation of simulated hydraulics

Simulated hydraulic conditions were compared to measured data from an acoustic doppler current profiler (ADCP) to validate the CFD model. Predicted resultant flow velocity increased with measured resultant flow velocity (Pearson's correlation test, $t = 4.362$, p value < 0.001, $r = 0.50877$), but there was a bias to the hydraulic model overestimating velocities at low measured velocities and underestimating velocities at high measured velocities. The hydraulic model was found to reproduce well the flow field in the study area.

2.6. Fish navigation and propulsion force estimation

We used fish thrust force to characterize different smolt swimming behaviours and to determine fish orientation at each fish position. Fish thrust force

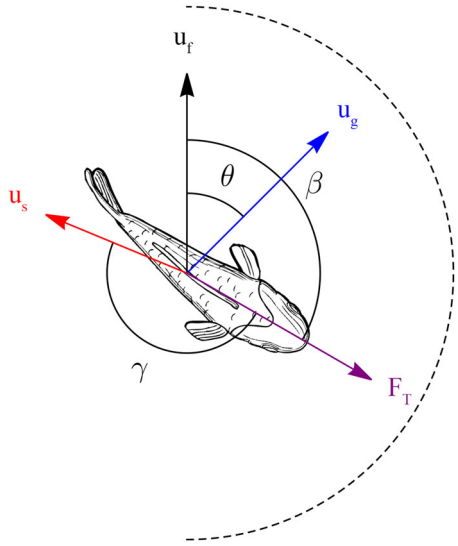

Figure 2. Smolt swim orientation and direction. Orientation is characterized by angle β between time-average flow velocity ($\vec{u}_f$) and fish thrust ($\vec{F}_T$) vectors. Direction is characterized by angle θ between time-average flow velocity ($\vec{u}_f$) and fish velocity with respect to the ground ($\vec{u}_g$). Relative direction is characterized by the angle γ between fish thrust ($\vec{F}_T$) and fish velocity with respect to the flow ($\vec{u}_s$).

quantifies the effort that the fish exerts upon the water to travel from one measured location to the next.

Thrust force and orientation describe more accurately how fish respond to what they perceive. Thrust force is evaluated by solving Newton's second law, following the approach of Arenas et al. (2015). Fish acceleration is given by the momentum equation:

$$m_{sm}\frac{d\vec{u}_g}{dt} = \vec{F}_D + \vec{F}_T, \tag{1}$$

where m_{sm} (kg), $\vec{u}_g$ (m/s), $\vec{F}_D$ and $\vec{F}_T$ (N) are the total fish mass, fish velocity with respect to the ground, fish drag and thrust force, respectively. Ground velocity, $\vec{u}_g$, and fish acceleration, $d\vec{u}_g/dt$ were calculated from fish positions measured by acoustic telemetry. A smoothing technique was applied to the measured fish positions to remove ground velocity values beyond swimming capacity. Videler (1993) defined this threshold as:

$$||\vec{u}_{g,max}|| = 0.4 + 7.4L_{sm} = 1.5\,\text{m/s}; \quad \text{where} \quad L_{sm} = 152\,\text{mm is smolt length.}$$

Values above $2||\vec{u}_{g,max}||$ were discounted as outliers, above smolt swimming capacity.

Equation 1 allowed us to calculate fish thrust, once $\vec{F}_D$ was known. Drag force was modelled as:

$$\vec{F}_D = -\frac{1}{2}\rho A_{sm} C_{d,sm}|\vec{u}_s|\vec{u}_s, \tag{2}$$

where ρ (kg/m^3) is the fluid density, A_{sm} (m^2) the smolt wetted area, $C_{d,sm}$ the drag coefficient and u_s the smolt velocity in relation to the flow (hereafter called swimming velocity). Swimming velocity was evaluated using the velocity composition relation: $\vec{u}_g = \vec{u}_s + \vec{u}_f$. Wetted surface was evaluated as:

$$A_{sm} = S_C L_{sm}^{S_e},$$

with $S_C = 0.28\,\text{m}^2$ a reference area and $S_e = 2.11$ a fitting constant (Webb 1976). The expression to calculate drag coefficient $C_{d,sm}$ depends on whether the fish is actively swimming or drifting with the flow. It is derived from the data of Webb et al. (1984):

$$C_{d,sm} = \begin{cases} \dfrac{493.9}{Re_{sm}^{0.922}} & \text{if swimming,} \\ \dfrac{0.072}{Re_{sm}^{0.2}} & \text{if drifting,} \end{cases} \tag{3}$$

where Re_{sm} corresponds to the smolt Reynolds' number defined as:

$$Re_{sm} = \rho|\vec{u}_s|\frac{L_{sm}}{\mu},$$

with μ (Pa s), ρ (kg/m^3) fluid dynamic viscosity and fluid density respectively. Note that this Reynolds' number is defined using $|\vec{u}_s|$ as fish velocity relative to the fluid.

Given the ground velocity and fish acceleration obtained from the telemetry and flow velocity data of the CFD simulations, we derived fish thrust by solving Equation 1. We solved this equation at each fish position i:

$$\vec{F}_T^{\,i} = m_{sm}\frac{\vec{u}_g^{\,i-1} - \vec{u}_g^{\,i}}{\Delta t} - \vec{F}_D^{\,i},$$

where Δt is the time interval between the two consecutive positions. We first assumed that the fish was swimming passively (i.e., drifting), as explained below. Then, if $|\vec{F}_T^{\,i}| < 6 \times 10^{-4}$ N, we went on to the next step, using passive drag.

Otherwise, we computed thrust force with active (i.e., swimming) drag.

Based on these fish thrusts, we defined three behavioural states: passive, endurance and burst. Following Arenas et al. (2015), we assumed that fish thrust 6×10^{-4} N corresponds to passive swimming: i.e., fish passively moving with the flow. This threshold corresponds to 10% of the fish thrust at the maximum sustained speed measured by Tang and Wardle (1992). Between 6×10^{-4} N and fish thrust at maximum sustained speed (6×10^{-3} N), fish were considered to be in an "endurance state". Maximum sustained speed corresponds to the maximum speed reachable in endurance swimming: i.e., an activity that can be maintained over a long period of time and uses only aerobic muscle fibers (Mu et al. 2019). Above the maximum sustained speed, the fish was in a "burst state". Burst swimming is swimming behaviour that cannot be maintained for a long time, that requires both aerobic and anaerobic muscle fibers, and can correspond to

Table 2. Ranges of hydraulic conditions intensities obtained by hierarchical clustering on principal components.

	Intensities			
Hydraulic conditions	Very low	Low	Medium	High
Time-average flow velocity (m / s)	$0.01 \leqslant u_f < 0.02$	$0.02 \leqslant u_f < 0.04$	$0.04 \leqslant u_f < 0.2$	$u_f \geqslant 0.2$
Flow acceleration (m/s^2)	$2 \times 10^{-6} \leqslant a_f < 4 \times 10^{-6}$	$4 \times 10^{-6} \leqslant a_f < 3 \times 10^{-5}$	$3 \times 10^{-5} \leqslant a_f < 3 \times 10^{-4}$	$a_f \geqslant 3 \times 10^{-4}$
TKE (m^2/s^2)	$4 \times 10^{-7} \leqslant k < 1 \times 10^{-6}$	$1 \times 10^{-6} \leqslant k < 3 \times 10^{-6}$	$3 \times 10^{-6} \leqslant k < 8 \times 10^{-5}$	$k \geqslant 8 \times 10^{-5}$

unsuitable predation conditions or breaking through water flow barriers (Mu et al. 2019).

2.6.1. Influence of hydraulic conditions on fish behaviour and corresponding navigation

The resulting dataset was composed of a set of rows, each row corresponding to a fish position, estimated fish thrust and associated fish behaviour and all the hydraulic factors at this point. To characterize fish orientation, we analyzed the angle β (Figure 2) between fish thrust and time-average flow velocity vectors. This determined fish orientation in relation to flow direction: i.e., head oriented upstream or downstream. Here we assumed that the fish thrust force direction corresponded to the fish direction. We also characterized fish swimming direction by the angle θ between fish ground velocity and time-average fluid velocity vectors. This determined how far fish followed the direction of the flow. In the smolt's frame of reference, we also described its relative swimming direction as the angle γ between fish thrust and velocity with respect to the flow (Figure 2). It allowed us to know fish swimming direction in their referential.

2.7. Data analysis

We analyzed how time-average flow velocity, flow acceleration and TKE (coming from 3D CFD model) influenced smolt thrust force, swimming orientation and direction at every measured fish position (coming from acoustic telemetry), with fish positions all pooled together.

These three hydraulic conditions were strongly positively inter-correlated: correlation coefficient $r^2 = 0.918$ for time-average flow velocity and TKE, $r^2 = 0.863$ for flow acceleration and time-average flow velocity and $r^2 = 0.849$ for flow acceleration and TKE. As such, it was not possible to disentangle their relative effects. In view of this, a principal component analysis of the three hydraulic variables was carried out, followed by hierarchical clustering on principal components to detect groups of similar hydraulic conditions in the dataset. This led us to distinguish four types hydraulic clusters: very low, low, medium or high intensity, as described in Table 2. Based on this, every fish positions is associated to a hydraulic condition intensity.

To assess the effect of hydraulic conditions intensities on smolt behaviour, we compared their distributions associated with each behavioural state and smolt swimming orientation and direction with respect to the flow. Kruskal-Wallis non-parametric tests were carried out to detect significant differences between distributions. This is a statistical test to determine whether differences between medians are significant.

3. Results

3.1. CFD simulations combined with smolt trajectories at Poutès

Figure 3 shows that for numerical simulations number 1, 2 and 3 most of the flow was directed toward the turbine intake. A maximum time-average flow velocity of about 0.3, 0.4 and 0.5 m/s respectively was observed near the turbine intake and bypass.

For numerical simulations number 4 and 5, there was very low time-average flow velocity (in average equal to 0.016 m/s, 0.034 m/s respectively) in the entire reservoir except at the bypass with time-average flow velocity that could reach 0.3 m/s.

For numerical simulations number 1, 2 and 3 where time-average flow velocities are higher (in average equal to 0.12, 0.2 and 0.31 m/s respectively) the trajectories appeared to be much more straightforward and directed towards the bypass, whereas for numerical simulations number 4 and 5 (in average equal to 0.016 m/s, 0.034 m/s respectively) smolts displayed active exploratory behaviour in the forebay before finding a pathway. Indeed, smolts spent little time to move downstream for medium and high hydraulic conditions intensities (largely encountered in numerical simulations number 1, 2 and 3) with an average time of 12 (min/max = 8/15), 13 (min/max = 13) and 5 (min/max = 2/11) minutes respectively. While for low hydraulic conditions intensities (largely found in numerical simulations number 4 and 5), smolts needed a significant amount of time to travel through the reservoir with an average time of 6 h (min/max = 3 minutes/13 hours) and 24 h (min/max = 13 minutes/3 days) respectively.

3.2. How do smolt behave depending on hydraulic conditions intensities?

The swimming behaviours were significantly different depending on hydraulic condition intensities (Table 3) ($\chi^2 = 88.171$, p-value < 0.001). Table 3

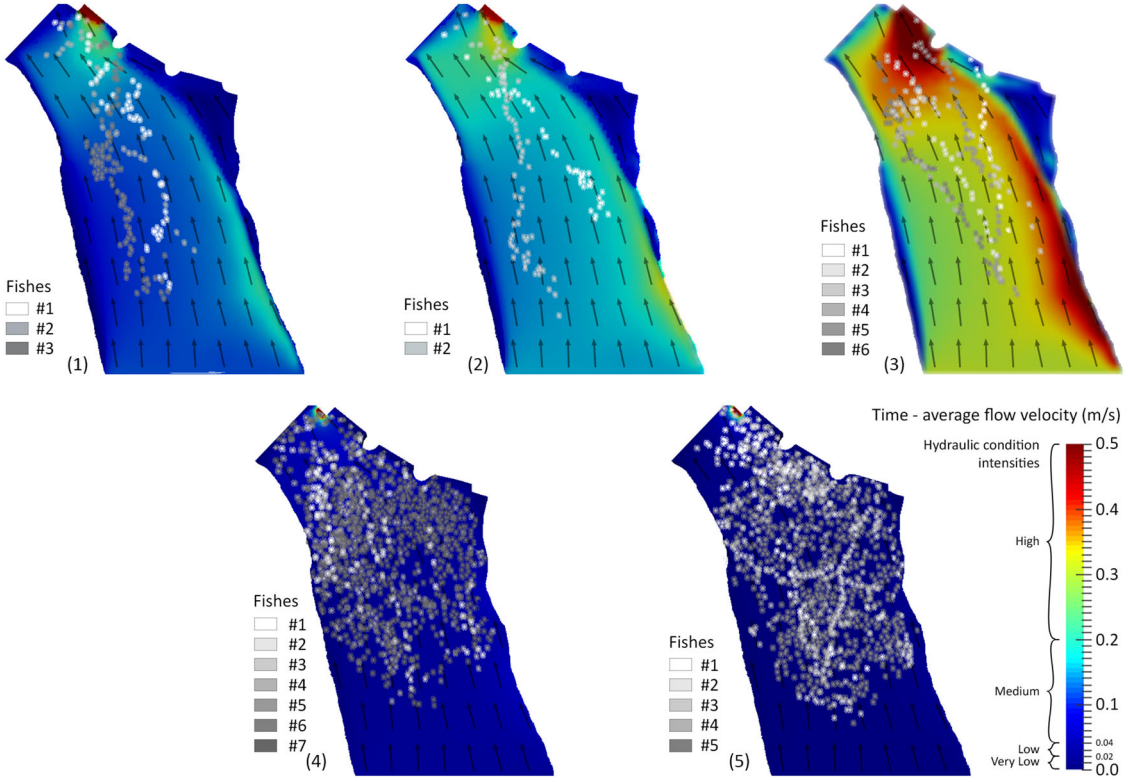

Figure 3. Five numerical simulations (time-average velocity for a water depth of 11 m for numerical simulation 1, 2 and 3 and 15.7 m for numerical simulation 4 and 5) combined with smolt trajectories at Poutès. The succession of a fish position through time allows the reconstruction of trajectories. The different colours for the fish positions correspond to different smolt's trajectory. Model input values (water level and discharges) of each numerical simulation are listed in Table 1.

Table 3. Proportion of the three swimming behaviours at Poutès dam for the different hydraulic conditions intensities (χ^2 test, $\chi^2 = 88.171$, p-value < 0.001).

	Passive swim $F_T < 6 \times 10^{-4}$ N	Endurance swim (Sustained swimming speed) $6 \times 10^{-4} \leqslant F_T < 6 \times 10^{-3}$ N	Burst swim (burst swimming speed) $F_T \geqslant 6 \times 10^{-3}$ N
Very low	1%	38%	61%
Low	3%	39%	58%
Medium	5%	57%	38%
High	8%	69%	23%

indicates that, for lower (very low and low) hydraulic conditions intensities, fish positions were mostly (respectively, 61% and 58%) in the burst swimming state. For higher (medium and high) intensities of hydraulic conditions, fish positions were mostly (respectively, 57% and 69%) in the endurance swimming state. The proportion of passively swimming fish positions was quite low, with not a significant difference between lower (1 to 3%) and the higher (5 to 8%) hydraulic intensities.

3.3. How do hydraulic conditions influence smolt's behaviour?

Figure 4 shows the influence of hydraulic conditions intensities on smolt swimming orientation β and thrust force (Figure 4a), and influence of hydraulic conditions on smolt swimming direction θ (Figure 4b).

Higher hydraulic conditions intensities were associated with lower fish thrust force (Figure 4). In low hydraulic conditions intensities, median thrust force was 7×10^{-3} N (burst swimming state) and decreased to 2.6×10^{-3} N (endurance swimming state) in high hydraulic conditions intensities.

In low hydraulic conditions intensities (Figure 4a1,2 and 4b1,2), fish orientation was erratic, leading to wide scatter in swimming angles. At intermediate level, thrust was also erratic (Figure 4a3), but swimming direction started to follow the flow direction (Figure 4b3), suggesting passive transport by the flow. At high intensity, fish navigated in the direction of the flow (Figure 4b4) but thrust was often orientated in the opposite direction with a low thrust force (Figure 4a4), suggesting controlled drift with the head facing flow direction. Statistical tests confirmed the influence of hydraulic conditions on fish thrust force (Kruskal-Wallis, $\chi^2 = 92.468$, p-value < 0.001), swimming orientation (Kruskal-Wallis, $\chi^2 = 13.728$, p-value < 0.01) and swimming direction (Kruskal-Wallis, $\chi^2 = 118.02$, p-value < 0.001).

(a)

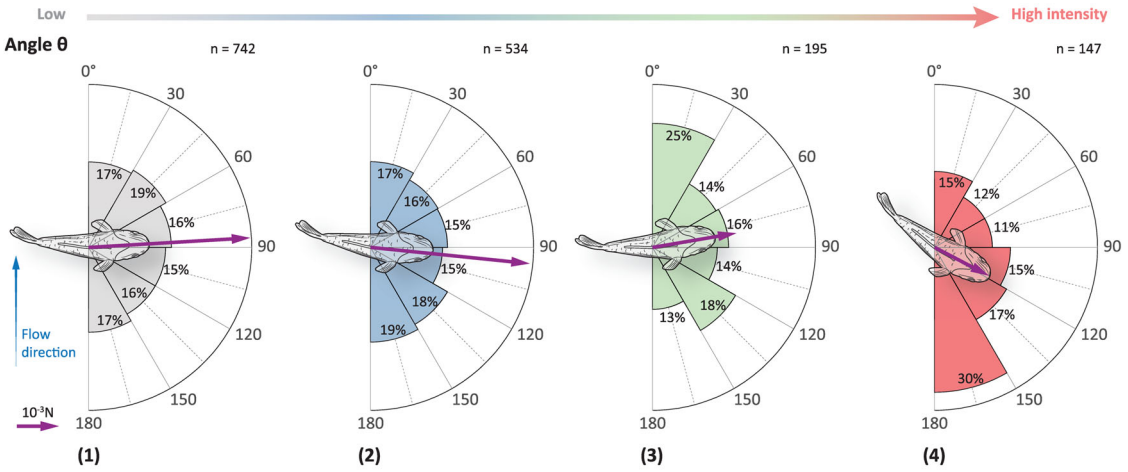

(b)

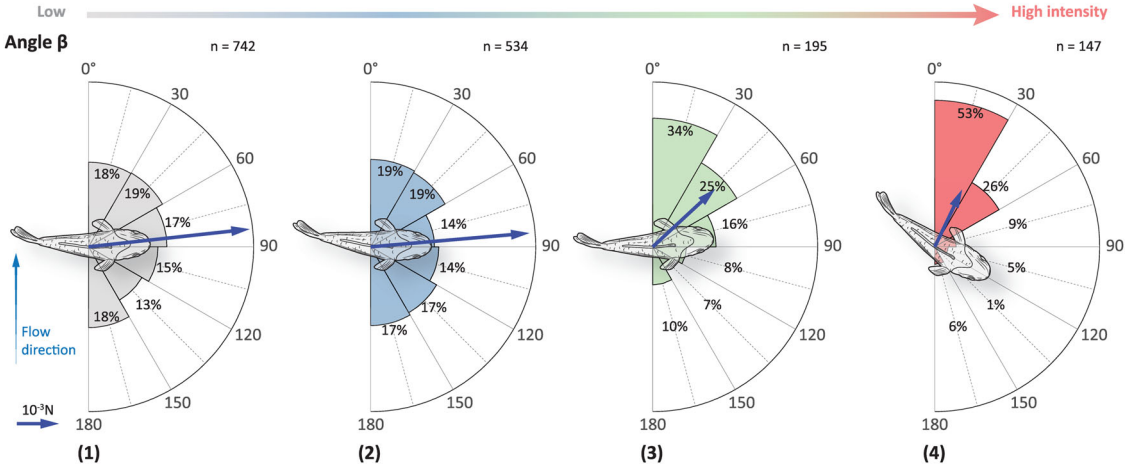

Figure 4. Influence of hydraulic condition intensities on smolt swimming orientation β and thrust force (a), and influence of hydraulic condition intensities on swimming direction θ (b). In each figure, the smolt position corresponds to median orientation. The purple arrow corresponds to the intensity of the fish thrust force (scale: 0.94 cm <- > 10^{-3} N). Figures 4a and 4b represents how very low (1), low (2), medium(3) and high (4) hydraulic condition intensities influenced swimming orientation, direction and thrust force.

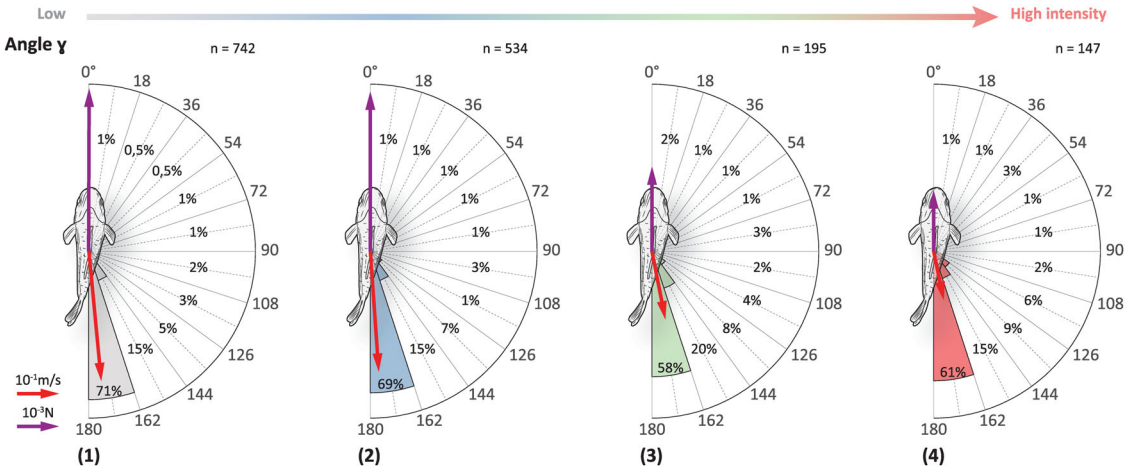

Figure 5. Influence of hydraulic condition intensities on relative swimming direction γ. The purple arrow corresponds to the intensity of the fish thrust force (scale: 0.94 cm <- > 10^{-3} N). The red arrow corresponds to the intensity of the fish velocity with respect to the flow (scale: 0.94 cm <- > 10^{-1} m/s).

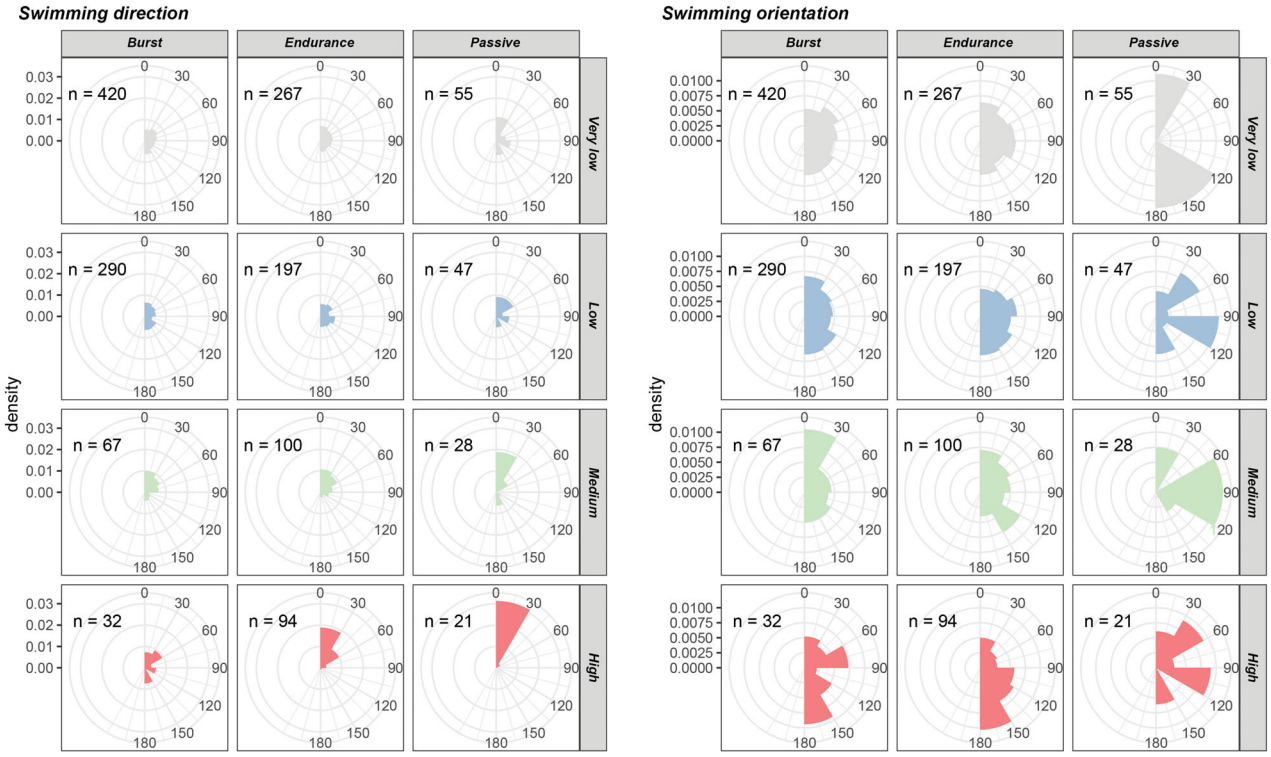

Figure 6. Smolt swimming orientation β (left) and direction θ (right) according to behavioural state and hydraulic condition intensity. Fish swimming orientation in relation to flow direction enabled to know if smolt had their head oriented upstream or downstream. And, fish swimming direction determined how far fish followed the direction of the flow.

Figure 5 shows the influence of the apparent flow velocity in the fish referential. According to Figure 5, smolt always swam against the apparent flow orientation. At low hydraulic conditions intensities, they induced this apparent flow direction with high thrust with a narrow range of apparent velocity angles. This implied that smolt were swimming straight ahead with little change of direction. At higher hydraulic conditions intensities, smolt thrust force decreased and the range of angles increased slightly. However, we did not observe any change in the distribution of relative swimming direction, regardless of the hydraulic conditions intensities (Kruskal-Wallis, $\chi^2 = 6.0704$, p-value $= 0.1082$).

3.4. How do smolt orient themselves according to their swimming behaviour?

Figure 6 completes Figure 4 by separating the orientations and directions by swimming behaviour. Smolts swam with the head facing the flow direction in a passive swimming state for low hydraulic conditions intensities (very low to low) and oriented in the same direction as the flow direction in a passive swimming state at higher hydraulic conditions intensities (medium to high).

In the endurance swimming state, at low hydraulic conditions intensities, smolts did not have a preferred swimming orientation or direction. Moreover, they swim mainly in burst swimming state with no preferred swimming orientation or direction for low hydraulic conditions intensities.

Smolts followed the direction of the flow, with the head in the same direction as the water flow at medium hydraulic condition intensity and with the head facing the water flow at high hydraulic condition intensity in a burst swimming state. However, they mainly swim in the same direction as the flow, oriented against the flow in an endurance swimming state for higher hydraulic conditions intensities (medium to high).

4 Discussion

4.1. Influence of flow velocity, flow acceleration and TKE on smolt behaviour

Based on 2D telemetry and a hydraulic model, it was possible to show that fish movements were well linked to hydraulic conditions intensity. A minimum time-average flow velocity threshold of 20 cm/s allowed them to move quickly through the reservoir.

The results showed that, at the Poutès dam, the stronger the hydraulic conditions, the lower the fish thrust. At relatively high time-average flow velocity, flow acceleration and TKE ($u_f \geqslant 0.2$ m/s, $a_f \geqslant 3\times10^{-4}$ m/s^2, $k \geqslant 8\times10^{-5}$ m^2/s^2), juvenile Atlantic salmon were in an endurance swimming state. They tended to move in the same direction as the flow, oriented against the flow. They were drifting.

The fact that fishes switch from negative (facing downstream) to positive rheotaxis (facing upstream) does not necessarily indicate that they want to move upstream, but is more likely a mechanism to increase escape readiness as needed, as hypothesized by Enders et al. (2009).

Under low hydraulic conditions intensity ($0.01 \leqslant u_f < 0.04$ m/s, $2 \times 10^{-6} \leqslant a_f < 3 \times 10^{-5}$ m/s^2, $4 \times 10^{-7} \leqslant k < 3 \times 10^{-6}$ m^2/s^2), smolt exhibited greater thrust force, and a burst swimming state predominated. They did not exhibit any predominant swimming orientation or direction; they seemed to be exploring the reservoir. As a result, they could remain in place for a long time and travel a long distance before passing through one of the dam surface outlets (water intake or bypass). In large reservoirs, flow patterns can be barely perceptible for fish, making them disoriented (Schwinn et al. 2019; Tétard et al. 2019).

Even if swim movement appears erratic, smolt were swimming straight ahead (i.e., maintaining their orientation with respect to the ground), which is a notable observation that will be important to consider when modelling smolt behaviour in a reservoir where hydraulic conditions intensities are very low.

Overall, juvenile Atlantic salmon upstream of the Poutès dam were mainly swimming actively. This is consistent with studies of smolt behaviour according to hydraulics upstream of a dam (Arenas et al. 2015; Johnson et al. 2000, 2009; Faber et al. 2001; Kemp et al. 2005, 2008).

Silva et al. (2020) analyzed how TKE and flow velocity influenced juvenile Atlantic salmon in the River Mandaselva, in Norway. They obtained three distinct behaviours: swimming in the same direction as the flow at a speed below their endurance state; diverging from the flow with higher swimming speeds; and swimming against the flow in a burst state. The first two behaviours were also found in the Poutès dam, but not the third.

According to the literature, swimming against the flow is observed at high hydraulic intensities (Arenas et al. 2015; Johnson et al. 2009; Enders et al. 2012), which are not found in reservoirs with low time-average flow velocity such as the Poutès dam. In such a reservoir, fish tend to explore the environment and then, when they detect sufficient flow, follow it.

Arenas et al. (2015) reported that the three species they had studied (chinook salmon, sockeye salmon and steelhead) exhibited average thrust forces of 1.4×10^{-2} N. This is very close to the thrust force of Atlantic salmon, which is 10^{-2} N, and it is interesting to compare the responses of the species to hydraulic cues. Pacific salmon showed a tendency to exert higher fish thrust as flow acceleration increases (for flow accelerations above 7×10^{-3} m/s^2), and Arenas et al. (2015) postulated a tendency of smolt to resist when flow acceleration increases. In Poutès, such levels of flow acceleration were never reached (maximum, 3×10^{-3} m/s^2) and fish never exhibited such resistive behaviour. However, Arenas et al. (2015) also noted that the thrust force for sockeye salmon and steelhead decreased for lower flow accelerations (between 4×10^{-3} and 7×10^{-3} m/s^2). This range of accelerations was also observed in Poutès, and the Atlantic salmon displayed the corresponding behaviour.

To ensure that smolt have optimal downstream migration conditions, there must be little TKE and a low upstream flow acceleration (Johnson et al. 2009; Goodwin et al. 2014). These two conditions, low TKE and low flow acceleration, apply at Poutès, which is a dam with particularly low time-average flow velocities in the reservoir, and can be assimilated to a reservoir with low flow fluctuations. The TKE is particularly low, with a maximum of 2.8×10^{-3} m^2/s^2. The same applies to flow acceleration, which reaches only 2×10^{-3} m/s^2. These hydraulic variables do not seem to interfere with smolt swimming motion.

Field and laboratory studies also corroborate this. Scruton et al. (2008) assessed bypass efficiency for juvenile Atlantic salmon at Bishop's Falls Dam in Canada, where forebay conditions are extremely turbulent. They compared the Bishop's Falls bypass efficiency (62–72%) to bypass efficiencies in facilities in the Eastern United States and Canada with less turbulent fluctuations in flow, and found that bypasses associated with less TKE had higher bypass efficiency (80–87%).

The aim of Odeh et al. (2002) experimental study was to improve the understanding of the effects of hydraulic turbulence intensity on juvenile fish; they created varying levels of turbulence intensity that resembled conditions found in the field, and concluded that, at low turbulence intensity, fish were able to swim and maintain vertical orientation.

Silva et al. (2020) reported that, in the main water course, smolts' relatively low TKE values (3×10^{-3} m^2/s^2) allowed them to maintain stability and swimming capacity.

Most studies analyzing fish behaviour during downstream migration were carried out in dams with very high hydraulic conditions intensities. This mainly results in recommendations concerning the upper limits of these parameters to improve the management of hydropower plants. However, we found results for very low time-average flow velocity, flow acceleration and TKE. And this did not seem to disturb smolt's swimming behaviour. When

time-average flow velocities are very low ($u_f < 2 \times 10^{-1}$ m/s) then it became very difficult for smolts to orient themselves. According to Coutant and Whitney (2000), low time-average flow velocity does not favour smolt orientation and leads to a decrease in migration speed.

4.2. Limitations and perspectives

The present study sheds light on swimming behaviour upstream of a dam according to several hydraulic conditions. However, since we had 2D telemetry data, we assumed that fish swim two meters below the water surface. This, knowing that according to studies on smolt's behaviour, they tend to swim close to the free surface (Coutant and Whitney 2000; Scruton et al. 2002; Gao et al. 2016). Ideally, 3D telemetry could be used and tracking devices optimized to achieve resolution similar to that of hydrodynamic models. Moreover, it was previously observed by Tétard et al. (2019), and McCormick (1998) that smolt behaviour changes with the period of migration. Therefore, the difference in swimming behaviour between hydraulic conditions intensities may be due to the timing of migration, which we did not take into account in our study. However, for the Poutès dam, the important concern is to have a relatively small reservoir to prevent migration delays (Tetard et al. 2016; Tétard et al. 2021). This is what is actually being undertaken for the dam's restoration.

Sensitivity analyses of the estimated forces with respect to positioning errors and errors of the CFD model should also be considered in order to achieve finer results than in this study, which should be considered as preliminary.

Despite the limited number of individuals considered in the analysis, the high temporal resolution of detection allowed us to have a data set with 1618 locations. However, since each individual was released in specific environmental conditions, there might be some confusions between inter-individual differences and environmental conditions. Ideally, a larger number of tagged individuals would have limited this risk but it was not possible to catch more wild fishes because of the status of the population (Dauphin and Prévost 2013). Farmed salmon had been used in the telemetry study to increase the number of individuals. First analysis by Tétard et al. (2021), did not detect any behavioural differences between wild and farmed salmons. Other authors found opposite results in other sites. Aarestrup et al. (1999) suggested that observed differences among wild and farmed salmon in migratory behaviour were related to genetic component. However, in the wild river, farmed salmons originate from local wild genitor and consequently are genetically similar to wild salmon. Nyqvist, McCormick, et al. (2017) did not see any behavioural difference between wild and hatchery fish while many studies reported differences between them (McCormick 1998; Thorstad et al. 2012). Given the observations of Tétard et al. (2021), the limited number of wild salmons and the genetic similarity between wild and farmed salmons, we did not explore for potential differences due to the origin of salmons.

Given that hydraulics is a key factor in fish behaviour (Nestler et al. 2008; Goodwin et al. 2014), the coupling of telemetry and CFD appears to be an appropriate approach. The framework proposed by Arenas et al. (2015) allowed rigorous coupling of the two data sources, enabling interpretation in terms of fish behaviour by comparison with experimental studies (although it would be preferable to carry out experiments under conditions strictly similar to those seen in the field). Fish thrust force and swimming orientation give us a precise description of smolt behaviour, revealing whether smolt swim with the head in the same direction as the water flow or with the head facing the water flow and to what extent they resist or do not resist the flow. Furthermore, this approach reveals precisely how fish react to what they perceive. This approach permits to establish behavioural rules that can then be used in fish trajectory prediction models, including the use of IBMs (Scheibe and Richmond 2002; Goodwin et al. 2006, 2014). This study paves the way for modelling approaches to simulate fish behaviour that go beyond Goodwin et al. (2014) by adjusting on observed data.

5. Conclusion

This paper presents a fine-scale analysis of smolts' behaviour in the forebay of a dam with particularly low time-average flow velocity, flow acceleration and TKE. Measured fish positions and CFD simulations were used to characterize smolt's swimming behaviour using fish thrust force, swimming orientation and direction. Thrust force was found by solving Newton's second law. The study aimed to analyze the effects of time-average flow velocity, flow acceleration and TKE on smolt's swimming behaviour. Our results showed that in spite of very low hydraulic conditions intensities in the reservoir that cause fish disorientation, a minimal time-average flow velocity of 20 cm/s in the reservoir was needed to guide smolts to the FPS. Results presented in this paper can be used to assess the impact of operational and/or structural modifications on fish attraction or dissuasion. The results could also be used to determine the hydraulic conditions

intensities that maximize fish drifting with the flow or swimming in the same direction as the flow.

Disclosure statement

No potential conflict of interest was reported by the authors.

ORCID

Hervé Capra http://orcid.org/0000-0002-3965-4314

References

Aarestrup K, Jepsen N, Rasmussen G, Okland F. 1999. Movements of two strains of radio tagged altlantic salmon, salmo salar l., smolts through a reservoir. Fishz Manag Ecol. 6(2):97–107.

Arenas A, Politano M, Weber L, Timko M. 2015. Analysis of movements and behavior of smolts swimming in hydropower reservoirs. Ecol Modell. 312: 292–307.

Baras E, Lucas MC. 2001. Impacts of man's modifications of river hydrology on the migration of freshwater fishes: a mechanistic perspective. Int J Ecohydrol Hydrobiol. 1(3):291–304.

Bleckmann H, Zelick R. 2009. Lateral line system of fish. Integr Zool. 4(1):13–25.

Braun CB, Coombs S. 2000. The overlapping roles of the inner ear and lateral line: the active space of dipole source detection. Phil Trans R Soc Lond B. 355(1401): 1115–1119.

Bunt C, Castro-Santos T, Haro A. 2012. Performance of fish passage structures at upstream barriers to migration. River Res Appl. 28(4):457–478.

Calles O, Olsson I, Comoglio C, Kemp P, Blunden L, Schmitz M, Greenberg L. 2010. Applied issues: Size-dependent mortality of migratory silver eels at a hydropower plant, and implications for escapement to the sea. Freshwater Biol. 55(10):2167–2180.

Coutant CC, Whitney RR. 2000. Fish behavior in relation to passage through hydropower turbines: a review. Trans Am Fish Soc. 129(2):351–380.

Cuinat R. 1988. Atlantic salmon in extensive french river system: Theb Loire-Allier. In: Atlantic salmon. Dordrecht: Springer; p. 389–399.

Dauphin G, Prévost E. 2013. Viability analysis of the natural population of atlantic salmon (salmo salar l.) in the allier catchment analyse de la viabilite d'une population naturelle de saumon atlantique.

Dijkgraaf S. 1963. The functioning and significance of the lateral-line organs. Biol Rev Camb Philos Soc. 38(1): 51–105.

Enders EC, Boisclair D, Roy AG. 2003. The effect of turbulence on the cost of swimming for juvenile atlantic salmon (salmo salar). Can J Fish Aquat Sci. 60(9): 1149–1160.

Enders EC, Gessel MH, Anderson JJ, Williams JG. 2012. Effects of decelerating and accelerating flows on juvenile salmonid behavior. Trans Am Fish Soc. 141(2): 357–364.

Enders EC, Gessel MH, Williams JG. 2009. Development of successful fish passage structures for downstream migrants requires knowledge of their behavioural response to accelerating flow. Can J Fish Aquat Sci. 66(12):2109–2117.

Evans SD, Adams NS, Rondorf DW, Plumb JM, Ebberts BD. 2008. Performance of a prototype surface collector for juvenile salmonids at bonneville dam's first powerhouse on the columbia river, oregon. River Res Appl. 24(7):960–974.

Faber DM, Weiland MA, Moursund R, Carlson TJ, Adams N, Rhondorf D. 2001. Evaluation of the fish passage effectiveness of the bonneville i prototype surface collector using three-dimensional ultrasonic fish tracking. Pacific Northwest National Lab.(PNNL), Richland, WA (United States). Report No:.

Fukushima M, Kameyama S, Kaneko M, Nakao K, Ashley Steel E. 2007. Modelling the effects of dams on freshwater fish distributions in Hokkaido, Japan. Freshwater Biol. 52(8):1511–1524.

Gao Z, Andersson HI, Dai H, Jiang F, Zhao L. 2016. A new eulerian–lagrangian agent method to model fish paths in a vertical slot fishway. Ecol Eng. 88:217–225.

Goodwin RA, Nestler JM, Anderson JJ, Weber LJ, Loucks DP. 2006. Forecasting 3-d fish movement behavior using a eulerian–lagrangian–agent method (elam). Ecol Modell. 192(1-2):197–223.

Goodwin RA, Politano M, Garvin JW, Nestler JM, Hay D, Anderson JJ, Weber LJ, Dimperio E, Smith DL, Timko M. 2014. Fish navigation of large dams emerges from their modulation of flow field experience. Proce Natl Acad Sci. 111(14):5277–5282.

Groux F, Therrien J, Chanseau M, Courret D, Tétard S. 2017. Shad upstream migration: Fishway design and efficiency.

Haefner JW, Bowen MD. 2002. Physical-based model of fish movement in fish extraction facilities. Ecol Modell. 152(2-3):227–245.

Haro A, Odeh M, Noreika J, Castro-Santos T. 1998. Effect of water acceleration on downstream migratory behavior and passage of atlantic salmon smolts and juvenile american shad at surface bypasses. Trans Am Fish Soc. 127(1):118–127.

Jansen HM, Winter HV, Bruijs MC, Polman HJ. 2007. Just go with the flow? Route selection and mortality during downstream migration of silver eels in relation to river discharge. ICES J Marine Sci. 64(7):1437–1443.

Johnson GE, Adams NS, Johnson RL, Rondorf DW, Dauble DD, Barila TY. 2000. Evaluation of the prototype surface bypass for salmonid smolts in spring 1996 and 1997 at lower granite dam on the snake river, washington. Trans Am Fish Soc. 129(2):381–397.

Johnson GE, Dauble DD. 2006. Surface flow outlets to protect juvenile salmonids passing through hydropower dams. Rev Fish Sci. 14(3):213–244.

Johnson GE, Richmond MC, Hedgepeth J, Ploskey GR, Anderson MG, Deng Z, Khan F, Mueller RP, Rakowski CL, Sather NK, et al. 2009. Smolt responses to hydrodynamic conditions in forebay flow nets of surface flow outlets, 2007. Pacific Northwest National Lab. (PNNL), Richland, WA (United States). Report.

Kalmijn AJ. 1989. Functional evolution of lateral line and inner ear sensory systems. In: The mechanosensory lateral line. New York, NY: Springer; p. 187–215.

Kemp PS, Gessel MH, Williams JG. 2005. Fine-scale behavioral responses of pacific salmonid smolts as they encounter divergence and acceleration of flow. Trans Am Fish Soc. 134(2):390–398.

Kemp PS, Gessel MH, Williams JG. 2008. Response of downstream migrant juvenile pacific salmonids to

accelerating flow and overhead cover. Hydrobiologia. 609(1):205–217.
Khan F, Johnson GE, Royer IM, Phillips NR, Hughes JS, Fischer ES, Ham KD, Ploskey GR. 2012. Acoustic imaging evaluation of juvenile salmonid behavior in the immediate forebay of the water temperature control tower at cougar dam, 2010. Pacific Northwest National Lab.(PNNL), Richland, WA (United States). Report.
Kondolf GM. 1997. Profile: hungry water: effects of dams and gravel mining on river channels. Environ Manage. 21(4):533–551.
Larinier M. 2001. Environmental issues, dams and fish migration. FAO Fish Tech Pap. 419:45–89.
Larinier M, Travade F. 2002. Downstream migration: problems and facilities. Bull Fr Pêche Piscic. 364: 181–207.
Li X, Deng ZD, Fu T, Brown RS, Martinez JJ, McMichael GA, Trumbo BA, Ahmann ML, Renholds JF, Skalski JR, et al. 2018. Three-dimensional migration behavior of juvenile salmonids in reservoirs and near dams. Sci Rep. 8(1):1–12.
Liao JC. 2007. A review of fish swimming mechanics and behaviour in altered flows. Philos Trans R Soc Lond B Biol Sci. 362(1487):1973–1993.
Liao JC, Beal DN, Lauder GV, Triantafyllou MS. 2003. Fish exploiting vortices decrease muscle activity. Science. 302(5650):1566–1569.
Limburg KE, Waldman JR. 2009. Dramatic declines in north atlantic diadromous fishes. BioScience. 59(11): 955–965.
Malmqvist B, Rundle S. 2002. Threats to the running water ecosystems of the world. Envir Conserv. 29(2): 134–153.
Marschall EA, Mather ME, Parrish DL, Allison GW, McMenemy JR. 2011. Migration delays caused by anthropogenic barriers: modeling dams, temperature, and success of migrating salmon smolts. Ecol Appl. 21(8):3014–3031.
McCormick MI. 1998. Behaviorally induced maternal stress in a fish influences progeny quality by a hormonal mechanism. Ecology. 79(6):1873–1883.2.0.CO;2]
Mogdans J. 2019. Sensory ecology of the fish lateral-line system: Morphological and physiological adaptations for the perception of hydrodynamic stimuli. J Fish Biol. 95(1):53–72.
Montgomery JC, Baker CF, Carton AG. 1997. The lateral line can mediate rheotaxis in fish. Nature. 389(6654): 960–963.
Montgomery JC, Coombs S, Baker CF. 2001. The mechanosensory lateral line system of the hypogean form of astyanax fasciatus. In: The biology of hypogean fishes. Dordrecht: Springer; p. 87–96.
Mu X, Cao P, Gong L, Baiyin B, Li X. 2019. A classification method for fish swimming behaviors under incremental water velocity for fishway hydraulic design. Water. 11(10):2131.
Neeson TM, Ferris MC, Diebel MW, Doran PJ, O'Hanley JR, McIntyre PB. 2015. Enhancing ecosystem restoration efficiency through spatial and temporal coordination. Proc Natl Acad Sci USA. 112(19):6236–6241.
Nestler J, Goodwin R, Smith D, Anderson J, Li S. 2008. Optimum fish passage and guidance designs are based in the hydrogeomorphology of natural rivers. River Res Appl. 24(2):148–168.
Noonan MJ, Grant JW, Jackson CD. 2012. A quantitative assessment of fish passage efficiency. Fish Fish. 13(4): 450–464.
Nyqvist D, Greenberg LA, Goerig E, Calles O, Bergman E, Ardren WR, Castro-Santos T. 2017. Migratory delay leads to reduced passage success of atlantic salmon smolts at a hydroelectric dam. Ecol Freshw Fish. 26(4): 707–718.
Nyqvist D, McCormick SD, Greenberg L, Ardren W, Bergman E, Calles O, Castro-Santos T. 2017. Downstream migration and multiple dam passage by atlantic salmon smolts. North Am J Fish Manage. 37(4):816–828.
Odeh M, Noreika JF, Haro A, Maynard A, Castro-Santos T, Cada GF. 2002. Evaluation of the effects of turbulence on the behavior of migratory fish. Final Report to the Bonneville Power Administration, Contract. :22.
Ovidio M, Dierckx A, Benitez JP, Nzau Matondo B, Philippart JC, Bernard B, Mandiki R, Evrard A, Kestemont P. 2016. Convention relative à la réhabilitation du saumon atlantique dans le bassin de la meuse (rapport 2015-2016).
Pedersen MI, Jepsen N, Aarestrup K, Koed A, Pedersen S, Økland F. 2012. Loss of european silver eel passing a hydropower station. J Appl Ichthyol. 28(2):189–193.
Porcher J, Travade F. 1992. Les dispositifs de franchissement: bases biologiques, limites et rappels réglementaires. Bull Français Pêche Piscicult. 326–327: 5–14.
R&D E. 2015. Code_Saturne 4.1.1 theory guide; [Online; accessed 2016 November 14]. http://code-saturne.org/cms/documentation.
Scheibe TD, Richmond MC. 2002. Fish individual-based numerical simulator (fins): a particle-based model of juvenile salmonid movement and dissolved gas exposure history in the Columbia river basin. Ecol Modell. 147(3):233–252.
Schwinn M, Baktoft H, Aarestrup K, Koed A. 2019. Artificial lakes delay the migration of brown trout salmo trutta smolts: a comparison of migratory behaviour in a stream and through an artificial lake. J Fish Biol. 94(5):745–751.
Scruton D, McKinley R, Kouwen N, Eddy W, Booth R. 2002. Use of telemetry and hydraulic modeling to evaluate and improve fish guidance efficiency at a louver and bypass system for downstream-migrating atlantic salmon (salmo salar) smolts and kelts. In: Aquatic telemetry. Dordrecht: Springer; p. 83–94.
Scruton D, Pennell C, Ollerhead L, Alfredsen K, Stickler M, Harby A, Robertson M, Clarke K, LeDrew L. 2008. A synopsis of 'hydropeaking'studies on the response of juvenile atlantic salmon to experimental flow alteration. Hydrobiologia. 609(1):263–275.
Silva AT, Baerum KM, Hedger RD, Baktoft H, Fjeldstad HP, Gjelland KØ, Økland F, Forseth T. 2020. The effects of hydrodynamics on the three-dimensional downstream migratory movement of atlantic salmon. Sci Total Environ. 705:135773.
Silva AT, Katopodis C, Santos JM, Ferreira MT, Pinheiro AN. 2012. Cyprinid swimming behaviour in response to turbulent flow. Ecol Eng. 44:314–328.
Silva AT, Santos JM, Ferreira MT, Pinheiro AN, Katopodis C. 2011. Effects of water velocity and turbulence on the behaviour of iberian barbel (luciobarbus bocagei, steindachner 1864) in an experimental pool-type fishway. River Res Applic. 27(3):360–373.
Steig TW, Johnston SV. 2010. Behavioral results from acoustically tagged fish using innovative techniques for analyzing three-dimensional data. In: OCEANS 2010 MTS/IEEE SEATTLE. IEEE. p. 1–11.

Strayer DL, Dudgeon D. 2010. Freshwater biodiversity conservation: recent progress and future challenges. J North Am Benthol Soc. 29(1):344–358.

Szabo-Meszaros M, Forseth T, Baktoft H, Fjeldstad HP, Silva AT, Gjelland KØ, Økland F, Uglem I, Alfredsen K. 2019. Modelling mitigation measures for smolt migration at dammed river sections. Ecohydrology. 12(7): e2131.

Tang J, Wardle C. 1992. Power output of two sizes of atlantic salmon (salmo salar) at their maximum sustained swimming speeds. J Exp Biol. 166(1):33–46.

Tarrade L, Texier A, David L, Larinier M. 2008. Topologies and measurements of turbulent flow in vertical slot fishways. Hydrobiologia. 609(1):177–188.

Tetard S, Lemaire M, De Oliveira E, Martin P. 2016. Use of 2d acoustic telemetry to study the behaviour of atlantic salmon smolts (salmo salar) approaching poutès dam (allier river, france). In: Proceedings of the 11th International Symposium on Ecohydraulics. p. 7–12.

Tétard S, Maire A, Lemaire M, De Oliveira E, Martin P, Courret D. 2019. Behaviour of atlantic salmon smolts approaching a bypass under light and dark conditions: Importance of fish development. Ecol Eng. 131:39–52.

Tétard S, Roy R, Teichert N, Rancon J, Courret D. 2021. Temporary turbine and reservoir level management to improve downstream migration of juvenile salmon through a hydropower complex. Knowledge and Management of Aquatic Ecosystems.

Thorstad EB, Økland F, Aarestrup K, Heggberget TG. 2008. Factors affecting the within-river spawning migration of atlantic salmon, with emphasis on human impacts. Rev Fish Biol Fisheries. 18(4):345–371.

Thorstad E, Whoriskey F, Uglem I, Moore A, Rikardsen A, Finstad B. 2012. A critical life stage of the atlantic salmon salmo salar: Behaviour and survival during the smolt and initial post-smolt migration. J Fish Biol. 81(2):500–542.

Thorstad EB, Havn TB, Saether SA, Heermann L, Teichert MAK, Diserud OH, Tambets M, Borcherding J, Økland F. 2017. Survival and behaviour of atlantic salmon smolts passing a run-of-river hydropower facility with a movable bulb turbine. Fish Manag Ecol. 24(3):199–207.

Timko MA, Brown LS, Wright CD, O'Connor R, Fitzgerald CA, Meager M, Rizor S, Nealson P, Johnston S. 2007. Analysis of juvenile chinook, steelhead, and sockeye salmon behavior using acoustic tags at wanapum and priest rapids dams, 2006. Final report by Hydroacoustic Technology, Inc, Seattle, Washington for Public Utility District. (2).

Videler JJ. 1993. Fish swimming. Vol. 10. Berlin: Springer Science & Business Media.

Vowles AS, Anderson JJ, Gessel MH, Williams JG, Kemp PS. 2014. Effects of avoidance behaviour on downstream fish passage through areas of accelerating flow when light and dark. Animal Behav. 92:101–109.

Webb PW. 1976. The effect of size on the fast-start performance of rainbow trout salmo gairdneri, and a consideration of piscivorous predator-prey interactions. J Exp Biol. 65(1):157–177.

Webb PW, Kostecki PT, Stevens ED. 1984. The effect of size and swimming speed on locomotor kinematics of rainbow trout. J Exp Biol. 109(1):77–95.

Williams JG, Armstrong G, Katopodis C, Larinier M, Travade F. 2012. Thinking like a fish: a key ingredient for development of effective fish passage facilities at river obstructions. River Res Appl. 28(4):407–417.